

Cambridge University Press

978-1-558-99372-3 - Gallium Nitride and Related Materials II: Symposium held April 1-4, 1997,
San Francisco, California, U.S.A.

C.R. Abernathy, H. Amano and J.C. Zolper

Excerpt

[More information](#)

Part I

Growth and Doping

Cambridge University Press

978-1-558-99372-3 - Gallium Nitride and Related Materials II: Symposium held April 1-4, 1997,
San Francisco, California, U.S.A.

C.R. Abernathy, H. Amano and J.C. Zolper

Excerpt

[More information](#)

Cambridge University Press

978-1-558-99372-3 - Gallium Nitride and Related Materials II: Symposium held April 1-4, 1997, San Francisco, California, U.S.A.

C.R. Abernathy, H. Amano and J.C. Zolper

Excerpt

[More information](#)

IMPURITY CONTAMINATION OF GaN EPITAXIAL FILMS FROM THE SAPPHIRE, SiC AND ZnO SUBSTRATES

Galina Popovici *, Wook Kim *, Andrei Botchkarev *, Haipeng Tang * James Solomon ** and Hadis Morkoç **

* University of Illinois at Urbana-Champaign, Coordinated Science Laboratory, 1101 West Springfield Avenue, Urbana, IL 61801

** Dayton Research Institute, Dayton, OH 45469-0167

* On leave at Wright Laboratory Wright Patterson AFB under a URRP program funded by AFOSR

ABSTRACT

Likely contamination of GaN films by impurities emanating from Al_2O_3 , SiC and ZnO substrates during growth has been studied by secondary ion mass spectrometry analysis. The highly defective interfacial region allows impurities to incorporate more readily as compared to the equilibrium solubility in a perfect crystal at a given temperature as evidenced by increased impurity levels in that region as detected by SIMS. The SIMS measurements in GaN layers grown on SiC and sapphire showed large amounts of Si and O, respectively, within a region wider than the highly disordered interfacial region pointing to the possibility of impurity diffusion at growth temperatures. The qualitative trend observed is fairly clear and significant. These observations underscores the necessity for developing GaN and/or AlN substrates.

INTRODUCTION

Wide band gap semiconductor materials extend the applications of semiconductors outside the realm of classical semiconductors such as Si and GaAs. [1-3] The large band gap, high thermal conductivity, and chemical inertness of nitrides pave the way for high power/temperature operation and light emission in green, blue and ultraviolet region of the spectrum. Of particular interest is the steady development of GaN technology in the last years, culminating in the demonstration of efficient green and blue light emitting diodes, and violet lasers.[4]

In spite of the rapid development many problems remain. The lack of an ideal substrate presents a major problem in GaN growth. Because of the high decomposition nitrogen pressure of GaN, no conventional crystal growth method can be employed to obtain bulk GaN crystals. Despite steady progress, GaN crystals grown from Ga solution under high pressure are not yet being produced in quantities needed, causing the growth efforts to heteroepitaxy on a variety of substrates, such as sapphire (Al_2O_3) [5], 6H-SiC [6], Si [7], GaAs [8], ZnO [9] and others, among which sapphire is the most widely employed one. Despite the poor lattice and thermal match, the best material grown today is on sapphire substrates. The preference towards sapphire substrates can be attributed to their ease of availability, hexagonal symmetry, and minimal pre-growth cleaning requirements. Sapphire is stable at high temperatures ($\sim 1000^\circ\text{C}$) required for epitaxial growth by vapor phase techniques. SiC (mismatch -3.4%) and ZnO (mismatch 2.0%) appear promising due to better lattice match compared to sapphire (mismatch

Cambridge University Press

978-1-558-99372-3 - Gallium Nitride and Related Materials II: Symposium held April 1-4, 1997, San Francisco, California, U.S.A.

C.R. Abernathy, H. Amano and J.C. Zolper

Excerpt

[More information](#)

-13%). ZnO has the best lattice match, but it decomposes at typical growth temperatures employed. Use of substrates other than GaN presents not only the inconvenience of the lattice and thermal mismatch, but also a possibility of unintentional contamination from the substrate during growth. While the influence of thermal and lattice mismatch from different substrates on GaN crystal structure and defect content have been studied extensively, possible contamination of GaN films by substrates during growth has not gotten much attention. In this paper, contamination of GaN films by impurity out-diffusion from Al_2O_3 , SiC and ZnO substrates during growth will be discussed. We show that the substrate may be a source of considerable contamination of the grown layer.

EXPERIMENTAL

GaN films were grown by reactive molecular beam (RMBE) details of which have been described elsewhere.[10] The temperature of the ammonia injector was kept at 300 °C. Two tandem Nanochem ammonia purifiers were utilized to reduce the oxygen level in ammonia. Basal plane sapphire substrates were degreased with organic solvents, and etched in a hot solution of H_2SO_4 and H_3PO_4 (H_2SO_4 : H_3PO_4 = 3:1) for 20 min. They were then rinsed with deionized(DI) water and blow dried with filtered nitrogen. Molten indium was then used to mount the sapphire substrates on Si templates mounted on molybdenum blocks with high purity carbon screws. Once in the growth chamber, nitridation was performed by exposing the sapphire substrate to an ammonia flux of 16 sccm for 1 min. at 850 °C. This nitridation condition was chosen as it provides the smoothest sapphire surface morphology. Growth temperature for both AlN buffer layer and GaN film was 800 °C. The thickness of the AlN buffer layers was 60 ~ 80 nm. The growth rate employed was about 0.7 $\mu\text{m/hr}$.

The depth profile of impurities along the growth direction was obtained by secondary ion mass spectroscopy(SIMS) performed using a CAMECA IMS-4f double focusing ion microanalyzer configured for cesium primary ion bombardment. The quantification of elemental concentration for this instrument was done by using relative sensitivity factors (RSFs) derived from the analysis of a GaN standard with known doses of impurity implants. The SIMS data near the surface (tens of nm) are in the limits of equilibration distance and should be disregarded. In addition, analyses were performed with 12kV oxygen and 10kV cesium with a quadrupole based instrument. No standards were available for quantification for this instrument.

RESULT AND DISCUSSIONS

Fig. 1 shows the SIMS depth profiles of impurities for the GaN layer grown on SiC. AlN buffer layer was used. One can see that Si is present near the interfacial layer, up to approximately 1/3 of the thickness, diffusing from the substrate. Moreover, concentration of oxygen and hydrogen is larger in this region as compared to the rest of the layer. O incorporates in the film from two sources: from the buffer layer and from the gas phase. H enters from the gas phase since ammonia is used as the nitrogen source. Al, Si and Ga profiles for the same sample, measured with the quadrupole instrument are shown in Fig. 2. These data are not quantitative, but a qualitative trend is clearly seen: Again, one can see that the concentrations of Al and Si are larger near the interface.

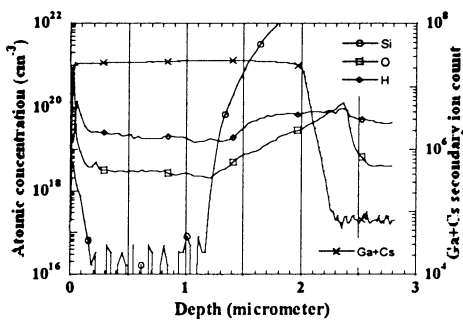


Fig. 1. The SIMS profile for Ga, Si, O, and H for the sample Grown on 6H-SiC. SIMS profiles were measured with a CAMECA IMS-4f double focusing ion microanalyzer. The data for Si are not quantitative.

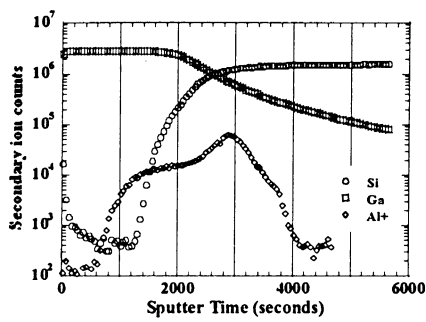


Fig. 2. The SIMS profile for Ga, Si, and Al for the same sample as in Fig. 1 measured with a quadrupole based instrument. The data are not quantitative.

Table I. Growth condition and the contamination depth of O, Si and Zn from Al₂O₃, SiC and ZnO substrates in the GaN films All samples were grown on AlN buffer layer.

Sample #	Substrate	T _{substrate} (°C)	Growth time (h)	Sample thickness (μm)	Measur. Impurity	Contam. depth (μm)
5465	Sapphire	800	2	2.5	Al	0.6
5536	Sapphire	793	2	0.8	O	0.30
5553	Sapphire	795	6	3.0	O	1.0
5554	Sapphire	800	6	3.0	O	1.0
5602	Sapphire	800	5	3.0	Al	1.0
					O	1.0
5550	SiC	810	6	2.0	Si	0.9
					Al	0.6
5518	ZnO	800	2	1.05	Zn	0.2
					O	0.2

It is well known that the presence of defects especially extended defects like dislocations, grain and twin boundaries, stacking faults and boundaries of the inversion domains enhance diffusion of impurities. The TEM studies of GaN films show that the region near the interface has the highest defect density compared to the region near the surface.[11-12] Therefore, one can expect that the amount of the impurities near the interface to be higher than it is permitted by the solubility limit of the perfect crystal.

The depth of contaminated layer depends on growth time as one can see from the Table I. From Table I it can be seen that the larger growth times result in larger impurities depths. The

Cambridge University Press

978-1-558-99372-3 - Gallium Nitride and Related Materials II: Symposium held April 1-4, 1997, San Francisco, California, U.S.A.

C.R. Abernathy, H. Amano and J.C. Zolper

Excerpt

[More information](#)

latter can be due to diffusion, since the thickness of the defective near-interface layer is set by lattice and thermal mismatch of the layer and substrate and should not significantly depend on the growth time, if the growth conditions are the same.

The results on contamination of the GaN layer from the substrate points to two stringent problems which hinder III-N research:

1. Lack of GaN substrates for the growth of GaN based devices.
2. Frequently in the existing literature, different deep levels are assigned to native defects, without taking into account contaminants, which could be responsible for deep levels as well.

CONCLUSIONS

The interfacial GaN layer near the substrate is contaminated during growth by the impurities from the substrate. The thickness of the contaminated layer is larger for longer growths.

ACKNOWLEDGMENTS

The research is funded by grants from ONR(contract #N00014-95-1-0635, #N00014-89-J-1780), AFOSR(contract #F49620-95-1-0298), under the supervision of Mr. M. Yoder, and Drs. G. L. Witt, Y. S. Park, and C. E. C. Wood.

REFERENCES

1. H. Morkoç Progress and Prospects of Group-III Nitride Semiconductors, International Symposium on blue Lasers and Light Emitting Diodes, Chiba Univ., Japan, March 5-7, 1996, p. 23-29.
2. S. N. Mohammad, A. Salvador, and H. Morkoç, Emerging Gallium Nitride Devices, Proc. IEEE v.83, 1306 (1995).
3. H. Morkoç, S. Strite, G. B. Gao, M. E. Lin, B. Sverdlov, and M. Burns, Large-band-gap SiC, III-V nitrides, and II-VI ZnSe-based Semiconductor Devices Technologies, J. Appl. Phys. 76, 1363 (1994).
4. I. Akasaki and H. Amano, Current Status of III-V Nitride Research, International Symposium on blue Lasers and Light Emitting Diodes, Chiba Univ., Japan, March 5-7, 1996, p. 11-16.
5. T. Lei, K. F. Ludwig, Jr., and T. Moustakas, J. Appl. Phys. 74, 4430 (1993)
6. M. E. Lin, S. Strite, A. Agarwal, A. Salvador, G. L. Zhou, N. Teraguchi, A. Rocket and H. Morkoç, Appl. Phys. Lett. 62, 702 (1993)
7. A. Ohtani, K. S. Stevens, and R. Beresford, MRS Symp. Proc. v.339, p.471-476.
8. J. W. Yang, J. N. Kuznia, Q. C. Chen, M. A. Khan, T. George, M. De Graef, and M. Mahajan, Appl. Phys. Lett. 67, 3759 (1995)
9. F. Hamdani, A. Botchkarev, W. Kim, H. Morkoç M. Yeadon, J. M. Gibson, S.-C. Y. Tsen, D. J. Smith, D. C. Reynolds, D. C. Look, K. Evans and C. W. Litton, Appl. Phys. Lett. 70, 467 (1997)
10. W. Kim, Ö. Aktas, A. E. Botchkarev, A. Salvador, S. N. Mohammad and H. Morkoç, J. Appl. Phys. 79, 7657 (1996).
11. Q. Zhu, A. Botchkarev, W. Kim, Ö. Aktas, A. Salvador, B. Sverdlov, H. Morkoc, S.-C.-Y. Tsen, and D. J. Smith, Appl. Phys. Lett. 68, 1141 (1996)
12. Z. Liliental - Weber, S. Ruvimov, T. Suski, J. W. Ager III, W. Swider, Y. Chen, Ch. Kisielowski, J. Washburn, I. Akasaki, H. Amano, C. Kuo, and W. Imler, MRS Symp. Proc. v. 423 (MRS, Pittsburgh, PA, 1996 p. 487.

Cambridge University Press

978-1-558-99372-3 - Gallium Nitride and Related Materials II: Symposium held April 1-4, 1997, San Francisco, California, U.S.A.

C.R. Abernathy, H. Amano and J.C. Zolper

Excerpt

[More information](#)

RELIABLE, REPRODUCIBLE AND EFFICIENT MOCVD OF III-NITRIDES IN PRODUCTION SCALE REACTORS

B. Wachtendorf, R. Beccard, D. Schmitz and H. Jürgensen

AIXTRON GmbH, Kackertstr. 15-17, D-52072 Aachen, Germany

O. Schön, M. Heuken

Institut für Halbleitertechnik I, RWTH Aachen, , Sommerfeldstr. 24, D-52074 Aachen, Germany

E. Woelk

AIXTRON Inc., 1569 Barclay Blvd., Buffalo Grove, IL 60089, U.S.A.

ABSTRACT

In this paper we present a class of MOCVD reactors with loading capacities up to seven 2" wafers, designed for the mass production of LED structures.

Our processes yield device quality GaN with excellent PL uniformities better than 1 nm across a 2" wafer and thickness uniformities typically better than 2%.

We also present full 2" wafer mapping data, High Resolution Photoluminescence Wafer Scanning and sheet resistivity mapping, revealing the excellent composition uniformity of the nitride compounds InGaN and AlGaIn. As well we will show sheet resistivity uniformity for Si-doped GaN and Mg-doped GaN.

INTRODUCTION

The worldwide demand for Ultra-High-Brightness blue and green LEDs has driven the development of MOCVD for Al-Ga-In-N alloy systems towards efficient multiwafer technology. We developed MOCVD reactors with loading capacities up to seven 2" wafers. The layers grown in these machines show excellent reproducibility from wafer to wafer and from run to run. The reactor design produces material with abrupt interfaces, even when using different substrates like Al_2O_3 , SiC, Si. As a standard tool for characterization we use non-destructive wafer topography, which is used to optimize the process for uniformity and yield.

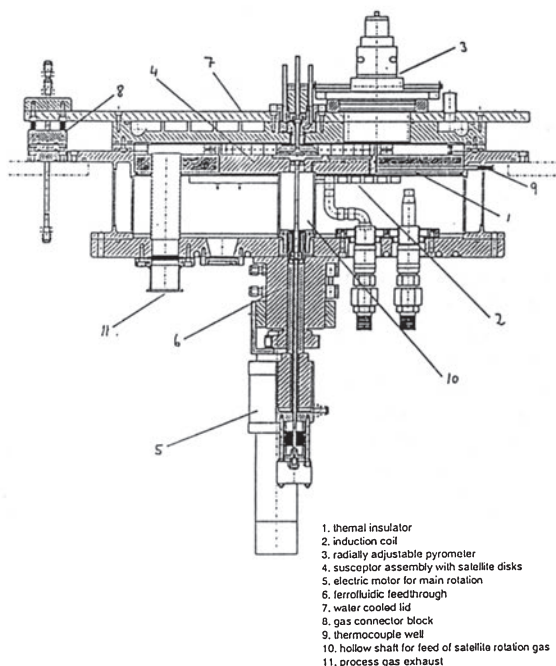


Fig. 1: cross section of the AIX2000HT Planetary Reactor

MOCVD REACTOR SYSTEMS

Key features of all the reactors are: Flexibility in the choice of the carrier gas in each single step of the structures, extremely low thermal mass allowing quick adjustment of different growth temperatures for each layer and real two-flow injection of the group III and group V reactants to minimize undesired prereactions. This also allows the process to be easily adapted from one machine to another.

Fig. 1 shows the cross section of the AIX2000 HT Planetary Reactor. The susceptor is heated by induction from the RF-coil which can be adjusted in height for the achievement of uniform temperature profiles. The low thermal mass of the susceptor allows steep cooling and heating ramps of about 5°C/s for the different process-steps. Like all AIXTRON reactors, the AIX2000HT is equipped with Gas Foil Rotation technology for the rotation of each substrate in addition to the rotation of the complete susceptor.

As it is well known that the nitride process is most sensitive to temperature fluctuations, special care was taken to design the coil in such a way that temperature gradients in the satellites are avoided. A pyrometer, which is mounted at the top of the reactor allows the continuous monitoring of the temperature through a purged viewport which can be used also for other in-situ measurement techniques like reflectivity based growth-rate determination. Fig. 2 shows a temperature measurement of a rotating planetary disk, with one SiC-wafer inside as a marker. This wafer is approx. 25°C colder than the empty satellites, so we can conclude that the temperature profile is better than 1°C within a 2" wafer. The MOCVD process is also designed to ensure maximum reliability and reproducibility. In particular, the initial deposition steps, which are commonly known to have a great influence on the layer quality have been optimized.

RESULTS

The standard tool for characterization is non-destructive wafer topography. It combines RT-PL-mapping, sheet resistivity mapping and also mapping of the layer thickness by white-light reflectometry.

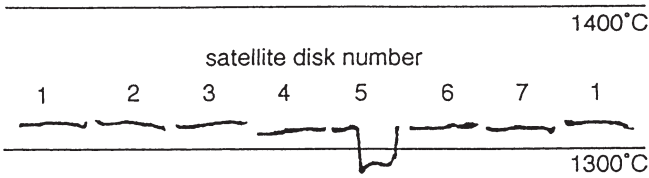


Fig. 2: temperature measurement of a planetary disk

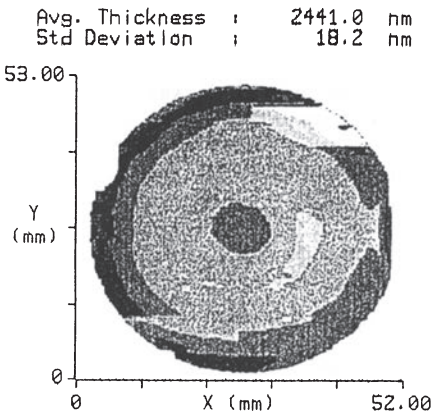


Fig.3: Thickness map of a GaN layer

This method has the following advantages:

- The characterization of the wafer is non-destructive, therefore it is not necessary to sacrifice wafers for characterization.
- The measurement is fast. No contacts or metallization are needed for thickness measurements or sheet resistivity mapping, which correspond to the doping profile. This means it is possible to receive fast feedback before device processing.
- The measurement is full automated and easy to use.

Our standard process for the growth of undoped GaN starts with a desorption step at elevated temperatures. After this a low-temperature GaN-nucleation layer is grown which will be annealed at high temperatures again. The GaN layer is grown on this nucleation layer. Depending on the parameters during nucleation and growth the material quality can be adjusted in a way that either background carrier concentrations below $1 \times 10^{17} \text{ cm}^{-3}$ are achieved or the layers are highly resistive.

Using the method of wafer mapping for characterization, we optimized the process in term of homogeneity and composition. Fig. 3 shows a thickness map of a very uniform GaN-layer. The standard deviation is below 0.8%, which is one of the best results ever reported for a full 2"-wafer. With an edge exclusion of 3mm the standard deviation is even better than 0.5%. The RT-PL map of this layer shows that the emission is very uniform across the full 2"-wafer (Fig. 4), the standard deviation of the peak wavelength is only 0.07nm, mostly due to noise.

Our processes yield doping uniformities better than 5% for Si-doping and better than 20% for Mg-doping. This can be verified with Hall-measurements, but this is a destructive method. It also takes some time to provide contacts, especially to the p-type material. For this reason we perform wafer mappings of sheet resistivity, which is directly related to the

Avg. Wavelength : 364.00 nm
Std Deviation : 0.066 nm

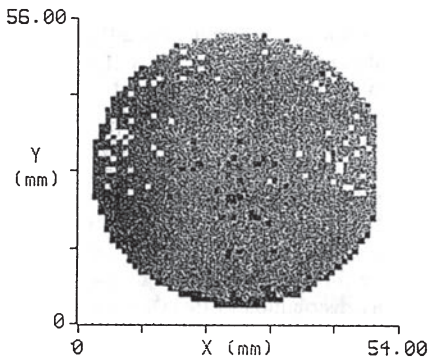


Fig. 4: Peak wavelength map of undoped GaN

Number of points : 25
Average measurement : 15.06 ohm/sq.
Max. value : 15.43 ohm/sq.
Min. value : 14.59 ohm/sq.
Variation in measurement : 5.556 %
Std. dev. from average : 0.25 ohm/sq.
Uniformity of wafer : 1.66 %

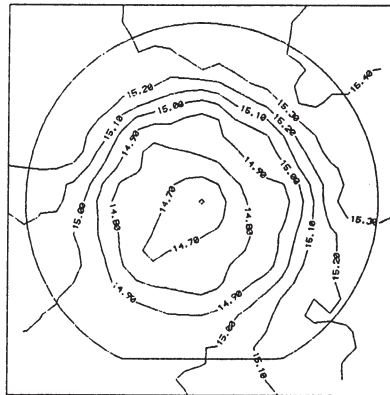


Fig. 5: sheet resistivity map of a Si:GaN-layer

doping level, taking the thickness uniformity into account. Fig. 5. shows the sheet resistivity map of a Si-doped GaN-layer. The standard deviation of the sheet resistivity is better than 2%. If we assume that the electron mobility is the same across the wafer, we can conclude that the doping level shows a uniformity better than 2% on the full wafer. The corresponding PL-Map shows a peak wavelength uniformity better than 0.25nm (Fig. 6).

For Mg-doping the sheet resistivity map shows a uniformity better than 20% after thermal activation of the holes (Fig. 7). This value is not as good as that for Si-doping because of interface effects between the GaN-buffer and the doped film and because of the more difficult thermal activation process of the holes.

InGaN MQW serves to adjust the wavelength of an LED. So the accurate adjustment of the concentration and PL-intensity distribution of InGaN are of major importance. Fig. 8 shows the peak wavelength distribution of a bulk InGaN-layer. The ultra high homogeneity in composition is reflected in the small standard deviation of the peak wavelength less than 0.75nm. The PL-intensity map of the same layer shows an intensity distribution in the range of 10% (Fig. 9). Both values fully meet the requirements of LED mass production.

The same applies to AlGaIn-layers. The production grade uniformity of the Al-GaN-composition is shown in Fig. 10, where the PL peak wavelength map is shown. The standard deviation of the average wavelength is of about 0.25nm, which meets all the requirements for the mass production of devices.

CONCLUSION

A new class of MOCVD reactors for the mass production of GaN-based optoelectronic devices was presented. We also presented uniformity data for doped and undoped GaN-layers as well as for the ternary alloys InGaN and AlGaIn. It was proven that the material quality is optimized for the production standards. The advantages of non-destructive wafer topography for statistical process control and also for process optimization were shown.

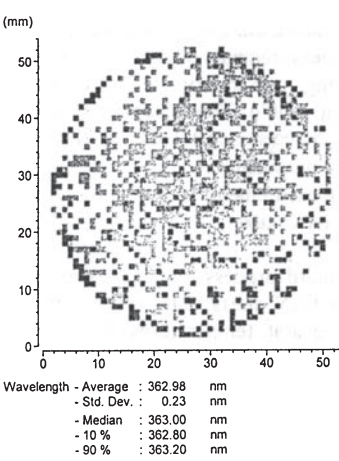


Fig. 6: RT-PL peak wavelength of a Si:GaN-layer

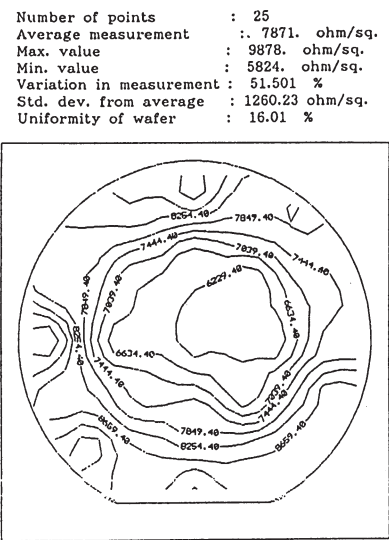


Fig. 7: Sheet resistivity map of a Mg-doped GaN layer